Physica B 407 (2012) 2176–2184

Contents lists available at SciVerse ScienceDirect

Physica B

journal homepage: www.elsevier.com/locate/physb

Modeling of the transient interstitial diffusion of implanted atoms during low-temperature annealing of silicon substrates

O.I. Velichko *, A.P. Kavaliova

Department of Physics, Belarusian State University of Informatics and Radioelectronics, 6, P. Brovki Str., Minsk 220013, Belarus

ARTICLE INFO

Article history:
Received 31 August 2011
Received in revised form
28 January 2012
Accepted 24 February 2012
Available online 3 March 2012

Keywords:
Diffusion
Annealing
Doping effects
Boron
Silicon

ABSTRACT

It has been shown that many of the phenomena related to the formation of "tails" in the low-concentration region of ion-implanted impurity distribution are due to the anomalous diffusion of nonequilibrium impurity interstitials. These phenomena include boron implantation in preamorphized silicon, a "hot" implantation of indium ions, annealing of ion-implanted layers et cetera. In particular, to verify this microscopic mechanism, a simulation of boron redistribution during low-temperature annealing of ion-implanted layers has been carried out under different conditions of transient enhanced diffusion suppression. Due to the good agreement with the experimental data, the values of the average migration length of nonequilibrium impurity interstitials have been obtained. It has been shown that for boron implanted into a silicon layer preamorphized by germanium ions the average migration length of impurity interstitials at the annealing temperature of 800 °C can be reduced from 11 nm to approximately 6 nm due to additional implantation of nitrogen. The further shortening of the average migration length is observed if the processing temperature is reduced to 750 °C. It is also found that for implantation of BF_2 ions into silicon crystal, the value of the average migration length of boron interstitials is equal to 7.2 nm for thermal treatment at a temperature of 800 °C.

1. Introduction

It is well known that boron is a basic impurity of p-conductivity used in the technology of the production of silicon integrated microcircuits [1]. Unfortunately, boron atoms have a small mass and large mobility in silicon crystals. Due to the small masses of boron ions, the formation of an amorphous layer in the ion-implanted substrates is not observed even at large fluencies. Only a great number of radiation defects are created. The absence of an amorphous layer and the presence of radiation defects result in the significant transient enhanced diffusion (TED) of ion-implanted boron during the subsequent annealing (see, for example, [2–20]). All these phenomena substantially complicate the problem of the formation of very shallow junctions with high electrophysical parameters. For suppressing the TED of ion-implanted boron, a method of boron implantation in a silicon layer preamorphized by heavier germanium ions is widely used [9,13–15,21–33]. Due to the solid phase epitaxial regrowth (SPER) of the amorphous layer, the region doped with boron is characterized by a perfect crystal structure, containing defects that are invisible by electron microscopy. However, the transient enhanced diffusion is observed as before, although it has another character and a smaller intensity. In Refs. [34,35] a qualitative difference of the form of boron profiles produced by annealing at temperatures of 800 °C and below was pointed out in comparison with the annealing at 900 °C and higher temperatures. Really, at low annealing temperatures an extended "tail" is observed in the low-concentration region of the impurity profile and the shape of this "tail" is a straight line if the axis of concentration is logarithmic. This feature of the boron distribution is observed even for "tail" extension compared to the characteristic size of the implanted region or smaller than it. At the same time, after annealing at a temperature of 900 °C or higher the shape of the boron profile for concentrations below approximately 10^8 μm^{-3} becomes convex upwards, i.e., similar to the Gaussian distribution. This behavior of the profile shape gives clear evidence of the change in the boron diffusion mechanism.

It is worth noting that the "tails" that represent a straight line, if the axis of concentration is logarithmic, are often observed directly after ion implantation of boron, phosphorus, gallium, and other impurity at room temperature (see, for example, Refs. [2,29] in the case of implantation of boron ions, Refs. [36,37] for phosphorus implantation, Refs. [38,39] in the case of implantation of gallium ions). The ion implantation in all the cases investigated was carried out in the direction deflecting from the crystal axis. According to Ref. [40], to completely remove the phenomenon of channeling and to eliminate the "tails" related to the scattering

* Corresponding author. Tel.: +375 296 998 078.
E-mail address: velichkomail@gmail.com (O.I. Velichko).

0921-4526/$ - see front matter © 2012 Elsevier B.V. All rights reserved.
doi:10.1016/j.physb.2012.02.036

of ions into channels, the ion implantation should be carried out in amorphous silicon. Nevertheless, later experiments show that "tails" are observed for boron implantation in the layers pre-amorphized by germanium ions [23,31].

For the low-temperature treatments of ion-implanted layers either an increase and broadening of existing "tails" in the bulk of a semiconductor occur or the formation of new "tails" if they are not observed after implantation. In the region of low impurity concentration, a "tail" represents as before a straight line for low-temperature annealing (i.e., for a small thermal budget). Really, an increase in the "tail" extension occurs during subsequent thermal treatments of preamorphized silicon layers that were implanted with boron ions [23,27,31,32]. In the investigations carried out by Refs. [15,22,28,33] clearly identified "tails" after boron implantation were not observed. However, such "tails" were formed in the course of the subsequent annealing. As follows from the experimental data of Ref. [41], a "tail" is also formed in the case of thermal treatment at 900 °C of silicon layers implanted with indium. This "tail" represents a straight line if the concentration axis is logarithmic. The experimental data also show that "tails" characterized by a straight line are often observed for the "hot" ion implantation of indium [41], gallium [41], antimony [42], and other impurities.

It was assumed originally that the formation of "tails" in the low-concentration region of ion-implanted impurity profiles, especially in the case of "hot" ion implantation, results from the fast diffusion of implanted impurity atoms [38,41–43]. It was supposed that impurity interstitials are this fast diffusing species [41,38,43]. For example, it was shown experimentally in Ref. [43] that during annealing of ion-implanted layers a significant fraction of indium and tellurium atoms leave their substitutional positions and become interstitials. The interstitial position is also a characteristic feature for atoms of gallium that, as well as boron, indium, and tellurium, is the element of III groups. However, in the latest papers [37,39] there are very serious arguments that the formation of "tails" in ion-implanted layers is related to the scattering of ions that reserved a part of the kinetic energy into channels. For example, in Ref. [37] phosphorus ions were implanted into thin silicon layers of different thicknesses. These layers were located on a substrate, which collected ions channeling through the layer. It was assumed that diffusing atoms do not have sufficient energy to leave the silicon crystal, whereas the channeling ions have. Experiments showed that the substrate really collects ions passed through the silicon layer. The doses of the passed ions were obtained as a function of the layer thicknesses. These doses correspond to the doses of phosphorus atoms in the region of the remainder of the "tail" for the investigated depth if ions were implanted in the continuous silicon. The results obtained were generalized in Ref. [39] for the cases of indium and gallium implantation. According to Ref. [39] the radiation-enhanced diffusion of gallium is impossible at room temperature. On the other hand, a characteristic "tail" is observed experimentally due to the scattering of ions into channels. Taking into account the possible annealing of damages and recovery of the crystal structure in the region of the end of the ion range, one can explain the results of Ref. [41] for "hot" high fluence implantation of indium and gallium ions without attracting the concept of an anomalous diffusion. Besides, at low temperatures a "tail" can be formed as a result of the channeling of a part of impurity atoms at the initial stage of implantation, when the amorphous phase was not formed as yet. Nevertheless, the mechanism of the "tail" formation is not clear until now, especially taking into account the latest experiments [23,31] related to boron implantation in the layer preamorphized by implantation of germanium ions. This allows us to formulate the following purpose of the research.

2. Main goal of the research

Not rejecting the possibility for a part of the ions of scattering into channels, we are to show that the long-range migration of nonequilibrium impurity interstitials is the main factor in the formation of "tails" in the region of low impurity concentration for random ion implantation into silicon crystals and implantation into preamorphized silicon layers.

3. Analysis of the mechanisms of the "tail" formation during ion implantation

Let us consider five characteristic cases of the formation of "tails" in the region of impurity concentration decreasing in the bulk of the semiconductor:

(i) "Tail" formation during the subsequent annealing of ion-implanted layers [41,15,22,28,33].
(ii) Formation of "tails" during ion implantation into amorphous silicon [23,31].
(iii) "Tail" formation during SPER of deposited amorphous Si layer doped with boron [44].
(iv) The phenomenon of "tail" formation during "hot" ion implantation [41,42].
(v) Formation of "tails" during ion implantation in the direction deflecting from the axis of the crystal at room temperature of the substrate [2,29,36–39].

It is evident that in the first three cases, there is no phenomenon of channeling and it is possible to explain the formation of "tails" only by the anomalous impurity diffusion. As an example, Fig. 1 presents the calculation of ion-implanted indium redistribution. The indium concentration profile was calculated within the framework of the model for diffusion of impurity interstitials described below. For comparison, the experimental data of Ref. [41] are used. In the work of Gamo et al. [41] the distributions of impurity atoms were obtained by measuring the γ-ray intensities in a combination with the layer removal technique. Indium was implanted with an energy of 45 keV to a dose of $\sim 1 \times 10^{15}$ ion/cm^2 and 8° off the $\langle 111 \rangle$ axis in order to reduce channeling effects. The temperature of annealing was 900 °C, and the thermal treatment duration was 20 min. The following values of parameters for the model of interstitial diffusion of ion-implanted impurity were used. The parameters of the as-implanted indium distribution are: $R_p = 0.03$ μm (30 nm); $\Delta R_p = 0.0084$ μm (8.4 nm); the parameters of the indium interstitial diffusion are: the

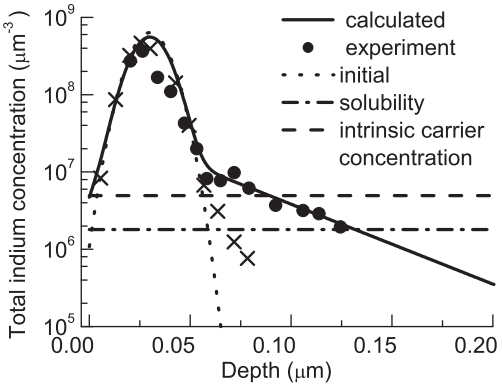

Fig. 1. Calculated indium concentration profile (solid line) after thermal treatment of implanted silicon substrate at 900 °C for 20 min. Gaussian distribution (dotted line) was used to approximate the initial impurity profile. The experimental data (× —impurity distribution after implantation; •—after annealing) are taken from Ref. [41] and the indium solubility limit is taken from Ref. [45].

average migration length of indium interstitials $l_{AI} = 0.042$ μm (42 nm); the time-average value of the generation rate of nonequilibrium impurity interstitials in the maximum of distribution $g_m^{AI} = 7.9 \times 10^4$ μm^{-3} s^{-1}. Here R_p and ΔR_p are the average projective range of impurity ions and straggling of the projective range, respectively. These parameters provide the best fitting of the calculated indium concentration profile to the experimental one.

As can be seen from Fig. 1, the results of calculation agree well with the experimental data. It is a very important argument in favor of the fast diffusion of nonequilibrium indium interstitials. Taking into account the good agreement with the experimental data, we use the model of the interstitial diffusion of ion-implanted impurity for simulating indium redistribution during "hot" ion implantation that was investigated in Ref. [41]. The results of simulation are presented in Fig. 2. The energy and the dose of indium ions are the same as in the previous experiment, namely, 45 keV and $\sim 1 \times 10^{15}$ ions/cm^2. The following value of the average migration length of indium interstitials was used for the best fit to the experimental data: $l_{AI} = 0.032$ μm (32 nm). This value is greater than the average migration length $l_{AI} = 0.027$ μm used for similar calculations in Ref. [46]. Perhaps, the increase of l_{AI} is due to the effect of evaporation of indium interstitials from the surface of the semiconductor [47] that we took into consideration in contrast to Ref. [46]. Taking into account the evaporation of indium interstitials made it possible to achieve the best agreement with the experimental profile in the vicinity of the surface.

It is seen from Fig. 2 that the results of calculation agree well with experimental data. The value of the average migration length for "hot" implantation of indium ions $l_{AI} = 0.032$ μm is close to the migration length $l_{AI} = 0.042$ μm for annealing of indium implanted layer at a temperature of 900 °C. It means that in the experiment with "hot" ion implantation a "tail" is also formed due to the fast migration of impurity interstitials. The results obtained suggested to revise the inferences drawn in Refs. [37,39] about "tail" formation due to the scattering of ions into channels. Really, these inferences were based on the experiments [37] with phosphorus ion implantation in thin silicon layers of different thicknesses. The main assumption of the above-mentioned paper is that diffusing phosphorus atom cannot pass through the boundary of the silicon crystal, while the ions which scatter into channels can cross the boundary due to the rest of the kinetic energy. However, within the framework of the interstitial diffusion model the "tail" formation is related to the diffusion of impurity interstitials. Therefore, there are no restrictions for impurity interstitials to evaporate from the surface of a crystal and then to collect on the substrate, on which the implanted layer is placed. This is confirmed by the experiments concerning hydrogen diffusion through thin silicon layers [48], because the extended "tails" on the hydrogen concentration profiles are also formed by interstitial diffusion [49].

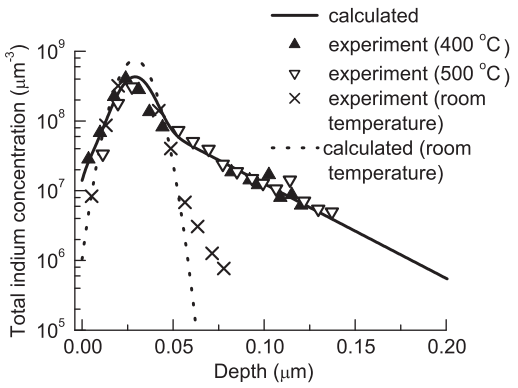

Fig. 2. Calculated indium concentration profile (solid line) after "hot" ion implantation. Gaussian distribution (dotted line) was used to approximate the concentration profile of indium atoms implanted at room temperature. The experimental data are taken from Ref. [41].

It is clear from the analysis carried out above that the vast majority of phenomena of "tail" formation in the low-concentration region of ion-implanted impurity profile is due to the fast impurity diffusion. The scattering of ions into channels can play only an auxiliary role in the experiments under investigation. It is usually supposed that impurity interstitials are the fast diffusing species [41,38,43,50]. Let us note that the mechanism of the long-range migration of nonequilibrium impurity interstitials was already used for explanation of gold diffusion in ion-implanted layers [51]. This mechanism was also used for describing "tail" formation during thermal treatments of the layers implanted with boron [50,52] and for explanation of boron diffusion in "buried" layers under the conditions of generation of nonequilibrium silicon interstitials [53,54]. Really, in Ref. [53] an analytical solution describing the redistribution of impurity atoms due to diffusion of boron interstitials during thermal treatment was obtained. As the initial condition for the distribution of boron atoms the δ-function was chosen. It was shown that for single participation of a boron atom in the act of interstitial migration a "tail" represents a straight line if the axis of concentration is logarithmic. It is necessary to note that the requirement of the occurrence of one event of impurity interstitial migration is realized in the models of the long-range migration of impurity interstitials proposed in Refs. [50,52,55]. On the other hand, under the condition of multiple migrations of the same impurity atom the boron profile has the form of Gaussian distribution [53]. Therefore, it was proposed in Ref. [54] to determine the microscopic mechanism of impurity transport by means of a change in the form of the impurity profile with increase in annealing duration. It is worth noting that the calculations which were carried out in Refs. [34,35,49,50,56] show that the "tail" representing a straight line is formed by the long-range migration of impurity interstitials not only in the case of initial distribution in the form of δ-function, but also for a generation rate of nonequilibrium interstitials described by the Gaussian distribution or any other distribution. Besides, the average migration length of impurity interstitials can be comparable with the characteristic size of the initial doped region, or even less than this size. It is worth noting that impurity diffusion can occur in an amorphous phase too, especially, if a high-current implanter is used for ion implantation and there is a possibility of substrate heating, as in the experiments of Cristiano et al. [23].

Let us consider boron diffusion in Si in more detail. It is well known that the diffusion of impurity atoms in silicon crystals can occur by a direct mechanism due to migration of impurity interstitials or by an indirect one as a result of the interaction with intrinsic point defects, namely, vacancies and self-interstitials [46,57,58]. It is usually supposed that substitutionally dissolved impurities diffuse by the indirect mechanism. For, example, it is well assessed that boron diffusion is governed by self-interstitials and the mobile B species is calculated to be the "boron atom–silicon self-interstitial" pair [59,60]. The situation is more complicated in ion-implanted layers and in the layers heavily doped during epitaxy. Indeed, in ion-implanted layers a significant amount of nonequilibrium self-interstitials are generated, which results in the transient enhanced diffusion of boron and other impurities diffusing due to the formation, migration and dissociation of the pairs with self-interstitials. On the other hand, a small fraction of impurity atoms can occupy the interstitial position after implantation. During annealing, these nonequilibrium impurity interstitials including interstitial boron atoms can diffuse by the direct mechanism without pair formation [50]. If the impurity

concentration is above the solubility limit, clustering of impurity atoms occurs. In this case, generation of nonequilibrium impurity interstitials can occur during cluster formation or dissolution [46,50]. These impurity interstitials also can migrate without pair formation. Moreover, the generation of impurity interstitials in these two cases (implantation or clustering) proceeds without direct interaction with silicon self-interstitials. It is worthy of note that in the models dealing with the pair diffusion mechanism the assumption of the local thermodynamic equilibrium between the substitutionally dissolved impurity atoms, nonequilibrium self-interstitials, and the pairs plays an essential part [46,57,58,61,62]. In this case, using the mass action law for the reactions of pair formation and reactions for charge state conversion of diffusing species, one can exclude, from the diffusion model, the equations that describe the migration of positively and negatively charged species. Thus, a set of diffusion equations written for diffusing species in each individual charge state is replaced by a fewer number of generalized equations [46,63,64]. As follows from Refs. [46,63,64], only concentrations of the neutral vacancies and self-interstitials are included in the generalized equation that describes impurity diffusion due to the pair formation mechanism. Moreover, the effective diffusivities of impurity atoms are the smooth and monotone functions of impurity concentration. It means that for uniform distributions of vacancies and self-interstitials in the neutral charge state, the equation of impurity diffusion is similar to the second Fick's law with the concentration dependent diffusivity [46]. In this case, the impurity concentration profiles after annealing have a usual convex form such as the Gaussian distribution. This form is in agreement with the majority of experimental data confirming the correctness of the local thermodynamic equilibrium. To explain the "tail" formation within the framework of the pair diffusion model, it is necessary to suppose the availability of the nonuniform distribution of point defects in the neutral charge state [46,63–65]. Using this assumption, one can explain the "tail" formation during high concentration phosphorus diffusion [46,64–67]. However, the boron concentration profiles in Si formed by TED during high temperature treatments are not characterized by "tails" in the low concentration region. It means that the distribution of self-interstitials in the neutral charge state is approximately uniform within the doped layer. On the other hand, after low temperature annealing the boron concentration profiles are often characterized by "tail" formation. Taking into account the experimental data for high temperature treatments, it is difficult to suppose that the distribution of self-interstitials in the neutral charge state is strongly nonuniform during low temperature annealing.

The other way of explaining "tail" formation within the framework of the pair diffusion mechanism follows from the results of Ref. [68] where it is shown that for the average migration length of the pairs $l_P \leq 0.05\Delta R_p$ the mass action law is valid in the concentration region from $10^{-3} \times C_m$ to C_m. Here C_m is the maximal value of impurity concentration at the peak of the Gaussian distribution. At the same time, the condition of local thermodynamic equilibrium can be disturbed in the low concentration region $C < 10^{-3} \times C_m$. Thus, to simulate the boron diffusion in the low concentration region, one needs two independent equations, namely, the conservation law for immobile substitutionally dissolved impurity atoms and the diffusion equation to describe the long-range migration of pairs. However, this mechanism of "tail" formation seems improbable for the simple reason. Indeed, the value of ΔR_p in the experiments under consideration is about 0.04 μm. It means that l_P should be smaller than 0.002 μm (2 nm) in the high concentration region. On the other hand, it follows from the experimental data that the average migration length of diffusing species in the "tail" region is approximately equal to 0.01 μm (10 nm), i.e., five times greater.

The straightforward way to explain the formation of "tails" is to take into account the long-range migration of nonequilibrium interstitial impurity atoms that are generated during cluster formation (dissolution) or have occupied interstitial positions after implantation. In the simplest case of such long-range migration one also needs two independent equations for impurity diffusion simulation: the conservation law for immobile substitutionally dissolved impurity atoms and the diffusion equation for mobile impurity interstitials. According to Ref. [55], a mathematical description of diffusion due to nonequilibrium "impurity atom – silicon self-interstitial" pairs or due to nonequilibrium impurity interstitials is identical. Therefore, it is impossible to conclude from the simulation results which species is responsible for "tail" formation. Following the previous analysis, we prefer to explain the "tail" formation within the framework of the long-range migration of interstitial impurity atoms. Indeed, for low temperature treatments of ion-implanted layers the diffusivity of the pairs is too small to provide a sufficient diffusion of impurity atoms despite the high concentration of nonequilibrium self-interstitials and, therefore, diffusion occurs due to the long-range migration of nonequilibrium impurity interstitials. On the other hand, for temperatures of approximately 900 °C and above, the redistribution of ion-implanted boron is governed by the pair diffusion mechanism at high impurity concentrations and by migration of nonequilibrium boron interstitials in the low concentration region [34]. It is worthy of note that the experimental data of Ref. [44] concerning the silicon doping with boron via amorphous silicon (a-Si) layer deposition and solid phase epitaxy to crystallize the deposited a-Si layer show unambiguously that the generation of boron interstitials is a result of the processes which accompany the high concentration doping, i.e., cluster formation, rearrangement or dissolution, because there are no defects created by ion implantation. In the experiment under consideration, the deposition of a-Si layer on standard (001)-oriented silicon substrates was performed. The precursor used for Si deposition is trisilane (Si_3H_8) that presents low decomposition temperature and thus allows low thermal budget deposition. Doping of films was achieved by using codeposition of Si_3H_8 and diborane (B_2H_6). The carrier gas was purified hydrogen (H_2). The doping profiles into the layers were determined by the secondary-ion-mass spectroscopy (SIMS). The result obtained contradicts the work of Duffy et al. [69] demonstrating that boron diffuses at high concentrations during low temperature thermal annealing in preamorphized silicon and that boron atoms at concentrations as high as 2×10^8 μm^{-3} are highly mobile at 500 and 600 °C in a-Si, while in crystalline silicon (c-Si) the mobile boron concentration is at least two orders of magnitude lower at the same temperatures. In Fig. 3 the experimental boron concentration profile in the totally crystallized layer obtained by SPER at a temperature of 500 °C for 600 s [44] and the results of simulation of the long-range migration of boron interstitials during solid phase epitaxy are presented. A constant concentration of $\sim 2 \times 10^9$ μm^{-3} was found through the film [44]. It corresponds to the full incorporation of the nominal boron concentration. After total crystallization, the film appears as a single crystal (154 nm thick), in perfect epitaxy with the substrate and fully free of extended defect. The sheet resistance of the sample is equal to 37 Ω for a film thickness of 154 nm, which corresponds to the active boron concentration 3×10^8 μm^{-3}. This value is significantly higher than the solubility limit $C_{sol} = 1.604 \times 10^6$ μm^{-3} [70]. As can be seen from Fig. 3, the results of simulation agree well with the experimental boron profile, especially in the region of the "tail". The value of the average migration length of boron interstitials $l_{AI} = 0.12$ μm was used for fitting to the experimental concentration profile. It is worthy of note that the value of boron diffusivity via the pair diffusion mechanism is equal to 2.83×10^{-16} μm^2/s

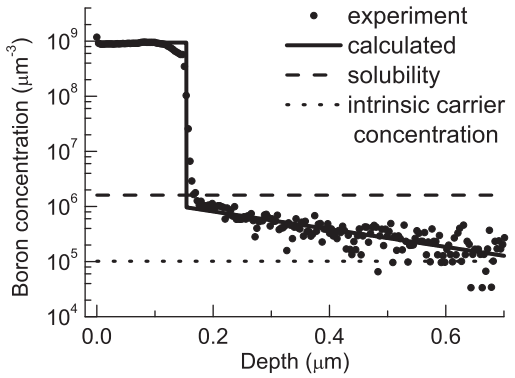

Fig. 3. Calculated boron concentration profile in silicon substrate after solid phase recrystallization (600 s at a temperature of 500 °C) of deposited a-Si layer doped uniformly with boron. The dashed curve represents boron solubility. The dotted line is intrinsic carrier concentration. The experimental data (filled circles) are taken from Ref. [44].

at a temperature of 500 °C [71]. This value of diffusivity corresponds to the average diffusion length of boron atoms for 600-s annealing $L = 4.12 \times 10^{-7}$ μm (4.12×10^{-4} nm) which is $\sim 300,000$ times smaller than the characteristic length of boron penetration into the silicon substrate. Thus, one can neglect the pair diffusion mechanism for such a low temperature annealing.

4. Model of interstitial diffusion

In Ref. [55], an equation for migration of nonequilibrium impurity interstitials was obtained which takes into account the different charge states of migrating species and also the drift of impurity interstitials in the built-in electric field and in the field of the elastic stresses. This equation has a form similar to the form of the equation describing the diffusion of nonequilibrium "impurity atom – intrinsic point defect" pairs when the influence of the built-in electric field and the field of the elastic stresses are also taken into account. As the mathematical formulations for the migration of nonequilibrium impurity interstitials and for the diffusion due to the nonequilibrium pairs are identical, it is impossible to make an exact conclusion about the kind of the mobile species from the form of impurity profile after thermal treatment. Let us consider for definiteness that boron transport during low-temperature annealing is carried out by migration of nonequilibrium impurity interstitials. We shall neglect the diffusion of the "impurity atom – intrinsic point defect" pairs in view of the small thermal budget. This assumption is based on the well-known opinion that impurity interstitials are the most mobile species. Taking into account that the extended "tail" is formed in the low-concentration region, where $C \le n_i$, we can suppose that the electric field does not influence the migration of impurity interstitials. Here C is the concentration of the substitutionally dissolved boron atoms; n_i is the intrinsic carrier concentration for the treatment temperature. It is clear that there is also no influence of the electric field in the case of migration of neutral interstitials even if $C > n_i$. We shall also neglect the influence of elastic stresses and suppose that substitutionally dissolved boron atoms and boron atoms incorporated into clusters and extended defects are immobile. Then, the system of equations describing redistribution of ion-implanted boron during low-temperature annealing has the following form:

(i) *The conservation law for immobile impurity atoms*:

$$\frac{\partial C^T(x,t)}{\partial t} = \frac{C^{AI}(x,t)}{\tau^{AI}} + G^{AS}(x,t), \tag{1}$$

(ii) *The equation of diffusion for nonequilibrium impurity interstitials*:

$$d^{AI}\frac{\partial^2 C^{AI}}{\partial x^2} - \frac{C^{AI}}{\tau^{AI}} + G^{AI}(x,t) = 0 \tag{2}$$

or

$$-\left[\frac{\partial^2 C^{AI}}{\partial x^2} - \frac{C^{AI}}{l_{AI}^2}\right] = \frac{\tilde{g}^{AI}(x,t)}{l_{AI}^2}, \tag{3}$$

where

$$l_{AI} = \sqrt{d^{AI}\tau^{AI}}, \quad \tilde{g}^{AI}(x,t) = G^{AI}(x,t)\tau^{AI}. \tag{4}$$

Here C^T is the total concentration of substitutionally dissolved impurity atoms and impurity atoms incorporated into clusters or trapped by extended defects (immobile impurity atoms): C^{AI} is the total concentration of nonequilibrium impurity interstitials in different charge states; d^{AI} and τ^{AI} are the diffusivity and the average lifetime of nonequilibrium impurity interstitials, respectively; G^{AI} is the generation rate of impurity interstitials. We use the stationary diffusion equation for impurity interstitials in view of their large migration length l_{AI} ($l_{AI} \gg l_{fall}$, where l_{fall} is the characteristic length of the decrease in the impurity concentration in the high-concentration region of impurity profile), and due to a small lifetime of these nonequilibrium interstitials τ^{AI} ($\tau^{AI} \ll \tau_p$, where τ_p is the duration of annealing). Let us note that the system of Eqs. (1) and (2) is similar to the systems of equations used in [51,52,50,53,54] for the description of interstitial diffusion.

To describe the spatial distribution of impurity atoms after implantation and spatial distribution of the generation rate of boron interstitials, the Gaussian distribution is chosen:

$$C_0(x) = C(x,0) = C_m \exp\left[-\frac{(x-R_p)^2}{2\triangle R_p^2}\right], \tag{5}$$

$$G^{AI}(x,t) = g_m^{AI} \exp\left[-\frac{(x-R_p)^2}{2\triangle R_p^2}\right], \tag{6}$$

where

$$C_m = \frac{Q}{\sqrt{2\pi}\Delta R_p} \times 10^{-8} \quad [\mu m^{-3}]. \tag{7}$$

Here C_m is the maximal concentration of impurity atoms after implantation; g_m^{AI} is the maximal value of generation rate of impurity interstitials per unit volume; Q is the dose of ion implantation [ion/cm^2]; R_p and $\triangle R_p$ are the average projective range of impurity ions and straggling of the projective range, respectively.

It is clear from expressions (5) and (6) that the model presupposes that the generation rate of boron interstitials is proportional to the total concentration of impurity atoms. Really, the analysis carried out in Ref. [50] shows that the boron interstitials can be generated during thermal treatment not only as a result of annealing of radiation defects, but also due to dissolution or rearrangement of the clusters that incorporated impurity atoms and also as a result of elastic stresses arising due to the small atomic radius of boron. This assumption is confirmed by the experimental data of Ref. [44], where the long-range migration of boron interstitials with the formation of the characteristic "tail" was observed during doping of the amorphous silicon layer deposited with the low thermal budget on a silicon substrate and then subjected to solid phase epitaxy. Thus, it follows from Ref. [44] that the long-range migration of boron interstitials is observed in the case of no radiation defects. As both the cluster concentration and intensity of elastic stresses are proportional to the total concentration of impurity atoms, the use

of expression (6) for describing the generation rate distribution of boron interstitials is quite reasonable.

5. Results of simulation of ion-implanted boron redistribution

In the case of the constant coefficients the system of Eqs. (1) and (3) allows obtaining an analytical solution. Such solutions for different boundary conditions on a finite interval $[0,x_F]$ within the assumption of continuous generation of impurity interstitials in the doped layer were obtained in Refs. [49,56]. We used these solutions for modeling the redistribution of ion-implanted boron. Let us note that the diffusivity d^{AI} has a constant value, if the migration of boron interstitials is not influenced by the built-in electric field. The average lifetime of these interstitials has a constant value in the case of absorption by the unsaturated traps distributed homogeneously in the bulk of a semiconductor. For example, such case of absorption is realized if replacement of the silicon atom by the boron interstitial from the lattice site to the interstitial one occurs.

Let us consider in the beginning the results of simulation of the experimental data of Ref. [33], because in this investigation various methods of the transient enhanced diffusion suppression were used. So, in Ref. [33] for suppression of the transient enhanced diffusion Czochralski grown (100) *n*-type silicon wafers were subjected to preamorphization by performing a germanium (Ge) ion implantation at 15 keV (Ge-PAI) and subsequently with 1 keV boron ions to a dose of 1.5×10^{15} cm^{-2}. Nitrogen (N) co-implantation to the same dose of 1.5×10^{15} cm^{-2} was performed on some wafers. The thermal annealing was carried out in a rapid thermal processing system under N_2 ambient at a temperature of 800 °C for 60 s. The dopant profiles were analyzed ex situ by SIMS. A cross-sectional TEM (XTEM) was also performed to analyze the extent of amorphization and the Ge-PAI induced EOR defects. The simulation of boron redistribution carried out for these conditions in Ref. [35] has shown good agreement with the experimental data for the average migration length of boron interstitials $l_{AI}=11$ nm. Also it was supposed that approximately 8.6% of the implanted boron atoms occupied interstitial positions. Migration of these nonequilibrium interstitial atoms results in the formation of an extended "tail" on the boron concentration profile. This "tail" is located in the interval from 0.02 μm up to approximately 0.1 μm from the surface of a semiconductor. For comparison Fig. 4 presents the results of modeling for the same process of ion-implanted boron redistribution in the case of additional nitrogen implantation at 6 keV after preamorphization due to germanium ions [33]. The energy of nitrogen implantation equal to 6 keV was chosen so that the maximum of N concentration was located between the boron doped region and a/c interface.

As can be seen from Fig. 4, there is good agreement between the calculated profile and the experimental data. The following values of the model parameters were used to provide the best fit of the calculated boron concentration profile to the experimental one: *quantities prescribing the initial distribution of implanted boron:* $R_p=0.0044$ μm (4.4 nm); $\Delta R_p=0.0036$ μm (3.6 nm). *Parameters specifying the process of interstitial diffusion:* the duration of annealing $\tau_p=60$ s; the annealing temperature $T=800$ °C; the average lifetime of nonequilibrium boron interstitials $\tau^{AI}=0.011$ s; the maximum value of the generation rate of nonequilibrium impurity interstitials $g_m^{AI}=6.7\times10^6$ μm^{-3} s^{-1}; the average migration length of boron interstitials $l_{AI}=5.9$ nm; the concentration of boron interstitials on the right boundary $C_F^{AI}=0$; the position of the right boundary $x_F=0.5$ μm. It was supposed that approximately 21% of the implanted boron atoms occupied the interstitial positions temporally.

As can be seen from the calculations performed, the additional implantation of nitrogen ions results in a significant (almost two times) reducing of the average migration length of boron interstitials. Therefore, the shrinkage of the "tail" approximately by 0.03 μm is observed that is very attractive from the technological point of view. It is worth noting that there is a significant (2.8 times) increase in the generation rate of boron interstitials. However, due to the reduced migration length of these interstitials, their main fraction is trapped within the implanted layer that does not result in an increase of the depth of $p-n$ junction. We assume that this trapping is due to the interaction with nitrogen atoms or with complexes of nitrogen and germanium atoms. It is worthy of note that the problem of interaction of boron interstitials with nitrogen and germanium atoms is complicated and requires further investigations. At present, our knowledge about this interaction is very poor.

A similar modeling for the case of transient enhanced diffusion suppression by using the lower annealing temperature, namely 750 °C, is presented in Fig. 5. *The following values of the parameters specifying the process of interstitial diffusion were used:* the maximum value of the generation rate of nonequilibrium impurity interstitials $g_m^{AI}=7.4\times10^6$ μm^{-3} s^{-1}; the average migration length of boron interstitials $l_{AI}=4.7$ nm. It follows from the values obtained that the decrease of the annealing temperature results in

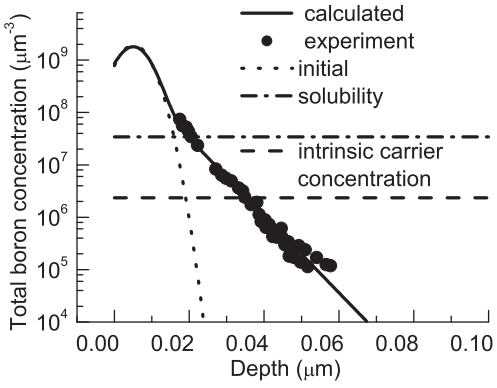

Fig. 4. Calculated boron concentration profile in silicon preamorphized by Ge ions after annealing for 60 s at a temperature of 800 °C. The dotted curve represents calculated boron distribution after ion implantation at an energy of 1 keV. An additional implantation of nitrogen ions at an energy of 6 keV for stronger suppression of the transient enhanced diffusion was carried out. The experimental data (filled circles) are taken from Ref. [33].

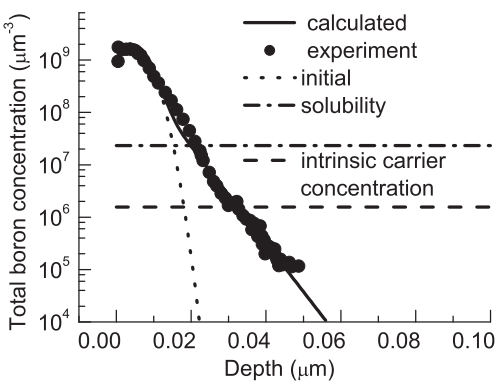

Fig. 5. Calculated boron concentration profile in silicon preamorphized by Ge ions after annealing for 60 s at a temperature of 750 °C. The dotted curve represents calculated boron distribution after ion implantation at an energy of 1 keV. An additional implantation of nitrogen ions at an energy of 6 keV for stronger suppression of the transient enhanced diffusion was carried out. The experimental data (filled circles) are taken from Ref. [33].

the reduction of the average migration length of boron interstitials and in the highly abrupt impurity profile.

Now, let us present the results of modeling the interstitial diffusion during boron implantation using the data obtained in Ref. [23]. In Ref. [23], *n*-type 10−20 Ω cm, prime (100) Si wafers were used. The wafers were first preamorphized with Ge ions (30 keV, 1×10^{15} cm^{-2}) to a depth of about 50 nm and then implanted with 0.5 keV boron ions to a dose of 1×10^{15} cm^{-2}. The implants were performed on a high-current implanter at tilt and twist angles of 0° with electrostatic deceleration in front of the target. The dopant atom distributions of all samples were analyzed using a high-resolution secondary ion mass spectrometry (SIMS). The boron concentration profile measured after implantation in preamorphized silicon is shown in Fig. 6. It is worth noting that due to the high-current implanter the wafer can be heated during ion implantation and migration of boron atoms can occur. Really, there is no channeling of ions due to implantation in the amorphous phase, whereas fast anomalous diffusion is quite possible in amorphous silicon.

As can be seen from Fig. 6, the curve calculated on the basis of the long-range migration of impurity interstitials agrees well with the measured boron concentration profile after implantation characterized by the extended "tail". The following values of the model parameters were used to provide the best fit of the calculated boron concentration profile to the experimental one: *quantities prescribing the Gaussian distribution of implanted boron:* $R_p = 0.0006$ μm (0.6 nm); $\Delta R_p = 0.0027$ μm (2.7 nm). *Parameters specifying the process of fast diffusion:* the maximum value of the generation rate of nonequilibrium impurity interstitials $g_m^{AI} = 3.2 \times 10^5$ μm^{-3} s^{-1}; the average migration length of boron interstitials $l_{AI} = 0.01$ μm (10 nm). For the best fit it was supposed that approximately 0.63% of the implanted boron atoms participated in the long-range migration.

Let us discuss the process of boron transport in amorphous silicon in more detail. A model of boron diffusion in a-Si was proposed in Ref. [72] where it is assumed that a boron atom jumps between adjacent threefold coordinated sites through temporarily restoring the metastable fourfold coordinated B, by the capture and release of one dangling-bond. In this paper, the experimental investigation and simulation of boron diffusion in a temperature range of 450–650 °C was also carried out. The experimental data show that boron diffusion occurs in the wide range of boron densities from very a low concentration up to a concentration of 10^{12} μm^{-3} [72] or less higher [69]. On the other hand, boron atoms in the region with the concentration above approximately 10^{12} μm^{-3} are immobile. Thus, the main feature of the boron concentration profiles after diffusion in a-Si is their qualitative similarity to the boron diffusion profiles in crystalline silicon formed by the pair diffusion mechanism when clustering occurs. It means that mobile species in a-Si diffuses according to Fick's law with concentration dependent diffusivity. Moreover, the local thermodynamic equilibrium is valid for substitutionally dissolved boron, dangling-bonds, and metastable boron atoms which capture the dangling-bonds. It is interesting to note that for the ion implantation under consideration this kind of diffusion is negligible because no change in the boron profile is observed in the concentration range from 10^{12} to 4×10^6 μm^{-3} (see Fig. 6). On the other hand, it follows from the experimental data of Ref. [23] that this mechanism of boron diffusion is realized for the greater thermal budget (for example, boron implantation and additional annealing of the ion-implanted layer at 650 °C for 5 s). This means that fast diffusion in the low concentration region below 4×10^6 μm^{-3} is not governed by boron interaction with dangling-bonds. We suppose that the "tail" formation in this region is due to the fast diffusion of impurity interstitials, and the experimental data of Ref. [23] can be explained on the basis of the long-range migration of nonequilibrium boron atoms.

However, there is also another way to explain the "tail" formation [73]. Really, the boron ions were implanted with electrostatic deceleration in front of the target. During the deceleration stage, some ions can become neutral due to reciprocal collisions. In such a case they will not be decelerated and keep their original energy. Due to the higher energy, these ions penetrate deeper in the bulk of the semiconductor. Therefore, this problem requires a further investigation.

Finally, in Fig. 7 the results of modeling of ion-implanted boron redistribution are shown, when the implantation of BF_2 ions was used for amorphization of the surface layer of silicon crystal and transient enhanced diffusion suppression [74]. In Ref. [74], (100) oriented, 10 Ω cm, *n*-type silicon wafers were subjected to BF_2 implantation at 2.2 keV to a dose of 1.0×10^{15} cm^{-2}. The furnace annealing was carried out at a temperature of 800 °C for 30 min. The resulting boron concentration profiles were measured by SIMS. The following values of the model parameters were used to provide the best fit of the calculated boron concentration profile to the experimental one: *quantities prescribing the initial distribution of implanted boron:* $R_p = 0.0002$ μm (0.2 nm); $\Delta R_p = 0.0014$ μm (1.4 nm). *Parameters specifying the process of interstitial diffusion:* the maximum value of the time-average generation rate of nonequilibrium impurity interstitials $g_m^{AI} =$

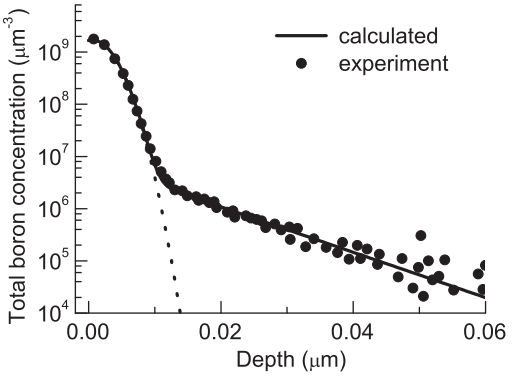

Fig. 6. Calculated concentration profile of boron implanted into silicon preamorphized by Ge ions. The long-range migration of boron atoms during implantation is taken into account. The dotted curve represents boron distribution after ion implantation at an energy of 0.5 keV calculated with no interstitial diffusion. The experimental data (filled circles) are taken from Ref. [23].

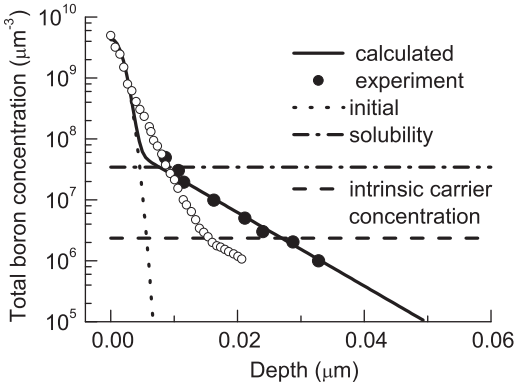

Fig. 7. Calculated boron concentration profile after annealing of a silicon layer implanted with BF_2 ions for TED suppression. Gaussian distribution (dotted line) was used to approximate the concentration profile of boron atoms after implantation (initial impurity distribution). The annealing was carried out for 30 min at a temperature of 800 °C. The experimental boron profiles (open circles after implantation and filled circles after annealing) are taken from the paper by Suzuki [74].

2.0×10^5 μm^{-3} s^{-1}; the average migration length of boron interstitials $l_{AI} = 0.0072$ μm (7.2 nm). It was supposed that approximately 4.1% of the implanted boron atoms occupied the interstitial positions temporally.

As is seen from Fig. 7, the calculated boron profile after furnace annealing agrees well with the experimental one in the "tail" region of impurity distribution that look like a straight line. It means that the "tail" region is formed due to the long-range migration of nonequilibrium boron interstitials. It is necessary to note that modeling of the experimental data obtained in Ref. [74] was carried out earlier in Ref. [75]. The model of Uematsu [76] was used for simulation of boron diffusion in Ref. [75]. It is supposed in this model that there is a local thermodynamic equilibrium between substitutionally dissolved boron atoms, silicon self-interstitials, and boron interstitials. It means from the microscopic point of view that the same boron atom becomes frequently interstitial, makes a number of chaotic jumps, and then becomes substitutionally dissolved again due to the "kick-out" of silicon atom from the lattice site. According to Ref. [54], the impurity profile for this diffusion mechanism has a form of the Gaussian distribution. Really, the boron concentration profile calculated in Ref. [75] represents the Gaussian distribution and disagrees with the experimental data. On the other hand, as follows from the experimental data [74], the boron concentration profile after annealing for 1.5 h begins to get a convex form similar to the Gaussian distribution. Remaining within the framework of the model of the long-range migration, such a change in the form of impurity distribution can be explained by taking into account the significant increase in the boron concentration in the "tail" region. Really, if the impurity concentration is greater than the intrinsic carrier concentration n_i, the migration of charged boron interstitials is influenced by the built-in electric field. On the other hand, the increase of annealing duration can create appropriate conditions for intensive dissolution of the clusters and extended defects incorporating silicon self-interstitials. In turn the generation of nonequilibrium self-interstitials results in boron diffusion due to the generation, migration, and dissolution of the "boron atom – silicon self-interstitial" pairs. It is usually supposed (see, for example, Refs. [64,77–79]) that the local thermodynamic equilibrium prevails between substitutionally dissolved boron atoms, silicon self-interstitials, and the pairs. Therefore, the boron concentration profile formed due to the pair diffusion should look similar to the Gaussian distribution that agrees with the experimental data for large thermal budget. However, the final solution of this problem requires further careful investigations.

6. Discussion

It is interesting to compare the obtained values of the average migration length of boron interstitials l_{AI} with the previous literature data [1,54,80]. For example, it was found in Ref. [54] that $l_{AI} < 5$ nm at a temperature of 900 °C and $l_{AI} = 10$ nm at 625 °C with an uncertainty of about 1 nm, i.e., the value of l_{AI} increases with decrease in the annealing temperature. Moreover, the boron concentration profile is characterized by the Gaussian shape distribution for an annealing temperature of 900 °C, whereas at 625 °C a "tail" is observed. It was concluded from the simulation results that the kick-out mechanism is responsible for the boron diffusion [54]. In Refs. [1,80], boron redistribution during annealing under different background doping levels was studied experimentally, and simulation was made on the basis of the pair diffusion mechanism. It was supposed that a neutral complex of a boron atom with a silicon self-interstitial (BI) is a migrating species. It was obtained in Ref. [80] from the results of simulation that the average migration length of the pairs varies in the range from 1 nm to 4 nm with a changing in the ratio p/n_i. Here p is the hole concentration. These investigations were resumed in Ref. [1]. It was reaffirmed that the average migration length of the pairs depends on the background doping level and increases in the range 1–5 nm with a decreasing temperature. It is worthy of note that the results of paper [54] agree with the numerical evaluation mentioned above that for $l_P < 2$ nm the local thermodynamic equilibrium is valid for the main region of impurity profile, whereas in the low concentration region the mass action law can be disturbed.

Unfortunately, it is impossible to carry out a direct comparison of the values of l_{AI} obtained in this paper with the values of the average migration length found in Refs. [1,54,80], because different cases of boron diffusion were simulated. Indeed, this paper investigated transport processes under the conditions of a very small thermal budget when the boron redistribution due to the pair diffusion mechanism or kick-out mechanism is negligible. We also carried out simulation of the redistribution of ion-implanted boron in the conditions of transient enhanced diffusion suppression due to additional doping with germanium and nitrogen atoms. Therefore, the reduction of l_{AI} with a decreasing temperature can explain by the lower concentration of traps for boron interstitials at higher temperatures, because more intensive diffusion of nitrogen and germanium atoms occurs. This problem requires further investigation.

7. Conclusions

We have shown that many cases of the formation of extended "tails" in the low-concentration region of ion-implanted impurity profiles, including ion implantation in the preamorphized silicon, "hot" ion implantation, impurity redistribution during the subsequent low-temperature annealing of ion-implanted layers, is related to the fast impurity diffusion. The channeling of ions scattered into channels is negligible for all the phenomena under consideration. With this purpose, simulation of indium redistribution during the subsequent annealing of ion-implanted layers and during "hot" indium implantation has been carried out. Many cases of the "tail" formation under different conditions of transient enhanced diffusion suppression during low-temperature annealing of boron implanted layers have been also investigated, including boron implantation into silicon preamorphized by germanium ions. The impurity concentration profiles calculated within the framework of the model of the long-range migration of nonequilibrium impurity interstitials agree well with experimental data. On this basis the values of the average migration length of nonequilibrium impurity interstitials have been obtained. So, if for boron implantation in silicon crystals preamorphized by germanium ions, the average migration length of boron interstitials is equal to 11 nm at an annealing temperature of 800 °C, the additional nitrogen implantation allows one to reduce this value approximately to 6 nm. A further reduction of the average migration length of boron interstitials can be achieved by decreasing the annealing temperature to 750 °C. Finally, for BF_2 implantation in silicon crystals the average migration length of boron interstitials is equal to 7.2 nm at an annealing temperature of 800 °C.

The characteristic feature of all the processes simulated in this paper is a very small thermal budget. Therefore, the diffusion mechanisms usually used for simulating the impurity redistribution during annealing, for example, so-called pair diffusion mechanism, do not change the impurity concentration profile. At the same time, the temperature of the substrate is enough to provide a long-range migration of interstitial impurity atoms. Simulation of "tail" formation for doping with indium and boron atoms, i.e., impurities substitutionally dissolved in the silicon lattice, reveals the second characteristic feature of the processes

under consideration. The fact is that a small fraction of these impurity atoms occupies temporally an interstitial position after ion implantation or due to cluster formation, rearrangement or dissolution. As a result, due to the long-range migration of these nonequilibrium impurity interstitials, extended "tails" in the low concentration region of impurity profiles are formed.

References

[1] D. De Salvador, E. Napolitani, G. Bisognin, M. Pesce, A. Carnera, E. Bruno, G. Impellizzeri, S. Mirabella, Phys. Rev. B. 81 (2010) 045209.
[2] W.K. Hofker, Philips Res. Repts. Suppl. 8 (1975) 1.
[3] A.E. Michel, W. Rausch, P.A. Ronsheim, R.E. Kastl, Appl. Phys. Lett. 50 (1987) 416.
[4] D. Fan, J. Huang, R.J. Jaccodine, P. Kahora, F. Stevie, Appl. Phys. Lett. 50 (1987) 1745.
[5] A.E. Michel, W. Rausch, P.A. Ronsheim, Appl. Phys. Lett. 51 (1987) 487.
[6] D.J. Eaglesham, P.A. Stolk, H.-J. Gossmann, J.M. Poate, Appl. Phys. Lett. 65 (1994) 2305.
[7] P.A. Stolk, H.-J. Gossmann, D.J. Eaglesham, D.C. Jacobson, C.S. Rafferty, G.H. Gilmer, M. Jaraiz, J.M. Poate, H.S. Luftman, T.E. Haynes, J. Appl. Phys. 81 (1997) 6031.
[8] W. Lerch, M. Glück, N.A. Stolwijk, H. Walk, M. Schäfer, S.D. Marcus, D.F. Downey, J.W. Chow, J. Electrochem. Soc. 146 (1999) 2670.
[9] K. Ohuchi, K. Adachi, A. Murakoshi, A. Hokazono, T. Kanemura, N. Aoki, M. Nishigohri, K. Suguro, Y. Toyoshima, Jpn. J. Appl. Phys. 40 (Part 1) (2001) 2701.
[10] S. Mirabella, A. Coati, S. Scalese, D. De Salvador, S. Pulvirenti, G. Bisognin, E. Napolitani, A. Terrasi, M. Berti, A. Carnera, A.V. Drigo, F. Priolo, Solid State Phenom. 82–84 (2002) 195.
[11] S.C. Jain, W. Schoenmaker, R. Lindsay, P.A. Stolk, S. Decoutere, M. Willander, H.E. Maes, J. Appl. Phys. 91 (2002) 8919.
[12] L. Shao, J. Liu, Q.Y. Chen, W.-K. Chu, Mater. Sci. Eng. R 42 (2003) 65.
[13] W. Lerch, S. Paul, J. Niess, S. McCoy, T. Selinger, J. Gelpey, F. Cristiano, F. Severac, M. Gavelle, S. Boninelli, P. Pichler, D. Bolze, Mater. Sci. Eng. B 124–125 (2005) 24.
[14] H. Graoui, M.A. Foad, Mater. Sci. Eng. B 124–125 (2005) 188.
[15] K.A. Gable, L.S. Robertson, A. Jain, K.S. Jones, J. Appl. Phys. 97 (2005) 044501.
[16] F. Lallement, D. Lenoble, Nuclear Instrum. Methods Phys. Res. Sect. B 237 (2005) 113–120.
[17] E.M. Bazizi, P.F. Fazzini, A. Pakfar, C. Tavernier, B. Vandelle, H. Kheyrandish, S. Paul, W. Lerch, F. Cristiano, J. Appl. Phys. 107 (2010) 074503.
[18] W.Y. Woon, C.L. Chen, Appl. Phys. Lett. 97 (2010) 121907.
[19] T. Philippe, S. Duguay, D. Mathiot, D. Blavette, J. Appl. Phys. 109 (2011) 023501.
[20] Y. Shimizu, H. Takamizawa, K. Inoue, T. Toyama, Y. Nagai, N. Okada, M. Kato, H. Uchida, F. Yano, T. Tsunomura, A. Nishida, T. Mogami, Appl. Phys. Lett. 98 (2011) 232101.
[21] S. Mirabella, D. De Salvador, E. Napolitani, F. Giannazzo, G. Impellizzeri, G. Bisognin, A. Terrasi, V. Raineri, M. Berti, A. Carnera, A.V. Drigo, F. Priolo, Nuclear Instrum. Methods Phys. Res. Sect. B 216 (2004) 80.
[22] R.A. Camillo-Castillo, M.E. Law, K.S. Jones, Mater. Sci. Eng. B 114–115 (2004) 312.
[23] F. Cristiano, N. Cherkashin, P. Calvo, Y. Lamrani, X. Hebras, A. Claverie, W. Lerch, S. Paul, Mater. Sci. Eng. B 114–155 (2004) 174.
[24] M.J.P. Hopstaken, Y. Tamminga, M.A. Verheijen, R. Duffy, V.C. Venezia, A. Heringa, Appl. Surf. Sci. 231–232 (2004) 688.
[25] B.J. Pawlak, R. Surdeanu, B. Colombeau, A.J. Smith, N.E.B. Cowern, R. Lindsay, W. Vandervorst, B. Brijs, O. Richard, F. Cristiano, Appl. Phys. Lett. 84 (2004) 2055.
[26] B.J. Pawlak, W. Vandervorst, A.J. Smith, N.E.B. Cowern, B. Colombeau, X. Pages, Appl. Phys. Lett. 86 (2004) 101913.
[27] B.J. Pawlak, R. Lindsay, R. Surdeanu, B. Dieu, L. Geenen, I. Hoflijk, O. Richard, R. Duffy, T. Clarysse, B. Brijs, W. Vandervorst, C.J.J. Dachs, J. Vac. Sci. Technol. B 22 (2004) 297.
[28] R.A. Camillo-Castillo, M.E. Law, K.S. Jones, L.M. Rubin, J. Vac. Sci. Technol. B 22 (2004) 312.
[29] M. Tomita, C. Hongo, M. Suzuki, M. Takenaka, A. Murakoshi, J. Vac. Sci. Technol. B 22 (2004) 317.
[30] R. Lindsay, K. Henson, W. Vandervorst, K. Maex, B.J. Pawlak, R. Duffy, R. Surdeanu, P. Stolk, J.A. Kittl, S. Giangrandi, X. Pages, K. van der Jeugd, J. Vac. Sci. Technol. B 22 (2004) 306.
[31] J.J. Hamilton, K.J. Kirkby, N.E.B. Cowern, E.J.H. Collart, M. Bersani, D. Giubertoni, S. Gennaro, A. Parisini, Appl. Phys. Lett. 91 (2007) 092122.
[32] M. Ferri, S. Solmi, D. Giubertoni, M. Bersani, J.J. Hamilton, M. Kah, K. Kirkby, E.J.H. Collart, N.E.B. Cowern, J. Appl. Phys. 102 (2007) 103707.
[33] S.H. Yeong, B. Colombeau, K.R.C. Mok, F. Benistant, C.J. Liu, A.T.S. Wee, G. Dong, L. Chan, M.P. Srinivasan, Mater. Sci. Eng. B 154 (2008) 43.
[34] O.I. Velichko, A.A. Hundorina, Materials and structures of modern electronics, in: V.B. Odzhaev, V.V. Petrov, V.A. Pilipenko, et al. (Eds.), Proceedings of IV International Conference, Belarusian State University, Minsk, Belarus, 2010, pp. 112–115. (in Russian).
[35] O.I. Velichko, A.A. Hundorina, Nonlinear Phenom, Complex Syst. 14 (2011) 384.
[36] R.A. Moline, J. Appl. Phys. 42 (1971) 3553.
[37] P. Blood, G. Dearnaley, M.A. Wilkins, J. Appl. Phys. 45 (1974) 5123.
[38] B.L. Crowder, J. Electrochem. Soc. 118 (1971) 943.
[39] G. Dearnaley, G.A. Gard, W. Temple, M.A. Wilkins, Appl. Phys. Lett. 27 (1975) 17.
[40] H. Ryssel, I. Ruge, Ion Implantation, 99th ed., John Wiley and Sons Inc, 1986.
[41] K. Gamo, M. Iwaki, K. Masuda, S. Namba, S. Ishihara, I. Kimura, I.V. Mitchell, G. Ilic, J.L. Whitton, J.A. Davies, Jpn. J. Appl. Phys. 12 (1973) 735.
[42] K. Gamo, K. Masuda, S. Namba, S. Ishihara, I. Kimura, Appl. Phys. Lett. 17 (1970) 391.
[43] J.A. Davies, L. Eriksson, J.W. Mayer, Appl. Phys. Lett. 12 (1970) 255.
[44] A. Gouyé, I. Berbezier, L. Favre, M. Aouassa, G. Amiard, A. Ronda, Y. Campidelli, A. Halimaoui, J. Appl. Phys. 108 (2010) 013513.
[45] S. Solmi, A. Parisini, M. Bersani, D. Giubertoni, V. Soncini, G. Carnevale, A. Benvenuti, A. Marmiroli, J. Appl. Phys. 92 (2002) 1361.
[46] O.I. Velichko, Ph.D. Thesis, Institute of Electronics of the National Academy of Sciences of Belarus, Minsk, 1988 (in Russian).
[47] I.C. Kizilyalli, T.L. Rich, F.A. Stevie, C.S. Rafferty, J. Appl. Phys. 80 (1996) 4944.
[48] A. Van Wieringen, N. Warmoltz, Physica 22 (1956) 849.
[49] O.I. Velichko, N.A. Sobolevskaya, Nonlinear Phenom. Complex Syst. 10 (2007) 376.
[50] O.I. Velichko, N.V. Kniazhava, Comput. Mat. Sci. 48 (2010) 409.
[51] M. Schulz, A. Goetzberger, Appl. Phys. 3 (1974) 275.
[52] O.I. Velichko, in: P. Grigaitis, C. Tamulevichyus (Eds.), Materials of the Seventh International Conference on Ion Implantation in Semiconductors and Other Materials, Vilnius, 1983, pp. 198–199 (in Russian).
[53] N.E.B. Cowern, K.T.F. Janssen, G.F.A. van de Walle, D.J. Gravesteijn, Phys. Rev. Lett. 65 (1990) 2434.
[54] N.E.B. Cowern, G.F.A. van de Walle, D.J. Gravesteijn, C.J. Vriezema, Phys. Rev. Lett. 67 (1991) 212.
[55] O.I. Velichko, Phil. Mag. 88 (2008) 1477.
[56] O.I. Velichko, N.A. Sobolevskaya, Nonlinear Phenom. Complex Syst. 14 (2011) 70.
[57] P.M. Faney, P.B. Griffin, J.D. Plummer, Rev. Mod. Phys. 61 (1989) 289.
[58] P. Pichler, Intrinsic point defects, impurities, and their diffusion in silicon, in: S. Selberherr (Ed.), Computational Microelectronics, Springer, Wien, New York, 2004.
[59] B. Sadigh, T.J. Lenosky, S.K. Theiss, M.-J. Caturla, T. Diaz de la Rubia, M.A. Foad, Phys. Rev. Lett. 83 (1999) 4341.
[60] W. Windl, M.M. Bunea, R. Stumpf, S.T. Dunham, M.P. Masquelier, Phys. Rev. Lett. 83 (1999) 4345.
[61] TSUPREM-4 User's Manual, Version 2000.4, Avant! Corp., Fremont, CA, 2000.
[62] I. Martin-Bragado, R. Pinacho, P. Castrillo, M. Jaraiz, J.E. Rubio, J. Barbolla, Mater. Sci. Eng. B 114–115 (2004) 284.
[63] O.I. Velichko, Yu.P. Shaman, A.K. Fedotov, A.V. Masanik, Comput. Mater. Sci. 43 (2008) 279.
[64] O.I. Velichko, Interaction of atomic particles with solid, in: I.I. Danilovich, A.G. Koval', V.A. Labunov, et al. (Eds.), Proceedings of VII International Conference, Part 2, Minsk Radioengineering Institute, Minsk, Belarus, 1984, pp. 180–181. (in Russian).
[65] O.I. Velichko, Elektronnaya tehnika. Ser. 2. Poluprovodnikovie pribory (Electronic Technics. Part 2. Semiconductor Devices). Issue 2(187) (1987) 85–87 (in Russian).
[66] M. Orlowski, Appl. Phys. Lett. 53 (1988) 1323.
[67] A.K. Fedotov, O.I. Velichko, V.A. Dobrushkin, J. Alloys Compd. 382 (1–2) (2004) 283.
[68] O.I. Velichko, Radiotekhnika i Elektronika (Radiotechnics and Electronics) Republican interdepartmental volume of papers, Minsk, Belarus, Issue 15 (1986), pp. 106–110 (in Russian).
[69] R. Duffy, V.C. Venezia, A. Heringa, B.J. Pawlak, M.J.P. Hopstaken, G.C.J. Maas, Y. Tamminga, T. Dao, F. Roozeboom, L. Pelaz, Appl. Phys. Lett. 84 (2004) 4283.
[70] S. Solmi, in: K.H.J. Buschow, R.W. Cahn, M.C. Flemings, B. Ilschner, E.J. Kramer, S. Mahajan, P. Veyssière (Eds.), Encyclopedia of Materials: Science and Technology, Elsevier Science Ltd., 2001, pp. 2331–2340.
[71] Y.M. Haddara, B.T. Folmer, M.E. Law, T. Buyuklimanli, Appl. Phys. Lett. 77 (2000) 1976.
[72] S. Mirabella, D. De Salvador, E. Bruno, E. Napolitani, E.F. Pecora, S. Boninelli, F. Priolo, Phys. Rev. Lett. 100 (2008) 155901.
[73] F. Cristiano, private communication.
[74] K. Suzuki, Solid-State Electron. 45 (2001) 1747.
[75] J. Marcon, A. Merabet, Mater. Sci. Eng. B 154–155 (2008) 216.
[76] M. Uematsu, J. Appl. Phys. 82 (1997) 2228.
[77] F.F. Morehead, R.F. Lever, Appl. Phys. Lett. 48 (1986) 151.
[78] D. Mathiot, S. Martin, J. Appl. Phys. 70 (1991) 3071.
[79] H. Bracht, Phys. Rev. B 75 (2007) 035210.
[80] D. De Salvador, E. Napolitani, S. Mirabella, G. Bisognin, G. Impellizzeri, A. Carnera, F. Priolo, Phys. Rev. Lett. 97 (2006) 255902.